Available online at www.sciencedirect.com
ScienceDirect
Journal of Solid State Chemistry 180 (2007) 3434–3442
JOURNAL OF SOLID STATE CHEMISTRY
www.elsevier.com/locate/jssc

Synthesis of Cd/(Al + Fe) layered double hydroxides and characterization of the calcination products

M.R. Pérez[a], C. Barriga[a], J.M. Fernández[a], V. Rives[b], M.A. Ulibarri[a,*]

[a]*Departamento de Química Inorgánica e Ingeniería Química, Campus de Rabanales, Universidad de Córdoba, Córdoba, Spain*
[b]*Departamento de Química Inorgánica, Universidad de Salamanca, Salamanca, Spain*

Received 30 May 2007; received in revised form 5 September 2007; accepted 29 September 2007
Available online 12 October 2007

Abstract

Layered double hydroxides (LDHs) containing Cd(II), Al(III), and Fe(III) in the brucite-like layers with different starting Fe/Al atomic ratios and with nitrate as counteranion have been prepared following the coprecipitation method at a constant pH value of 8. An additional Cd(II),Al(III)-LDH sample interlayered with hexacyanoferrate(III) ions has been prepared by ionic exchange at pH 9. The samples have been characterized by elemental chemical analysis, powder X-ray diffraction (PXRD), and FT-IR spectroscopy. Their thermal stability has been assessed by thermogravimetric and differential thermal analyses (TG-DTA) and mass spectrometric analysis of the evolved gases. The PXRD patterns of the solids calcined at 800 °C show diffraction lines corresponding to Cd(Al)O and spinel-type materials, which precise nature ($CdAl_2O_4$, $Cd_{1-x}Fe_{2+x}O_4$, or $Cd_xFe_{2.66}O_4$) depends on location and concentration of iron in the parent material or precursor.

Keywords: Hydrotalcite; Hexacyanoferrate; Layered double hydroxides; Differential thermal analysis; Mass spectroscopy

1. Introduction

Hydrotalcite-like compounds, also known as anionic clays or layered double hydroxides (LDHs), have the general formula $[M^{II}_{1-x}M^{III}_x(OH)_2]\,(A^{n-})_{x/n}\cdot mH_2O$. Metal cations are located in coplanar octahedra $[M(OH)_6]$ sharing edges and forming $M(OH)_2$ layers with the brucite (cadmium iodide-like) structure. Partial substitution of the divalent cations by trivalent ones gives rise to a positive charge in the layers, balanced by anions located between the hydroxylated layers, where water molecules also exist. A large number of LDHs have been synthesized [1–4], by changing the nature of the trivalent and divalent cations in the layers or through intercalation of a great variety of anions between the brucite-like layers, including simple inorganic (carbonate, nitrate, halides, etc.) and organic anions, as well as anionic complexes or polyoxometalates [5]. In the same way, it is possible to synthesize LDHs containing three or more cations in the layers.

Decomposition of LDHs at moderate temperatures leads to mixed oxides displaying high specific surface areas, good interdispersion of the metal cations, and reactivity, which are of interest because of their catalytic applications. Thermal decomposition [2] of LDHs containing carbonate or nitrate in the interlayer starts at 200–300 °C and proceeds through intermediate amorphous phases, whose structure is not well known. The final decomposition product is a mixture of $M^{II}M^{III}_2O_4$ spinel and $M^{II}O$ oxide because a M^{II}/M^{III} ratio larger than 1 is required to form a stable hydrotalcite and, therefore, the divalent cation is always in excess above the stoichiometry corresponding to the spinel. While the *M*O oxide is usually identified by powder X-ray diffraction (PXRD) for samples calcined at 600–700 °C, higher temperatures are required to record diffraction peaks ascribed to the spinel, and undetected trivalent cations are supposed [2] to be forming amorphous phases (M_2O_3 or spinel-like); alternatively they can be substituting isomorphically divalent cations in the *M*O phase, as in some cases the lattice parameters measured for the *M*O phase are slightly different from those reported for the bulk oxide. These systems can be appropriate

*Corresponding author.
E-mail address: maulibarri@uco.es (M.A. Ulibarri).

0022-4596/$ - see front matter © 2007 Elsevier Inc. All rights reserved.
doi:10.1016/j.jssc.2007.09.035

precursors in the synthesis of ferrites and other mixed oxides [6] useful for their magnetic properties, as well as for their role as mixed oxides for the catalytic production of olefins through oxidative dehydrogenation [7].

Hydrotalcite-like materials containing Cd^{II} and Al^{III}, Mg^{II} and Al^{III}, or Zn^{II} and Al^{III} in the brucite-like layers and nitrate in the interlayer [8–10], and the two last systems also with hexacyanoferrate as the interlayer anion [9,10], have been previously reported, studying the effect of the synthesis route on the purity of the materials and the crystalline phases formed were analyzed. Other materials containing Zn^{II}, Al^{III}, and Fe^{III} in the layers, with carbonate [11] or hexacyanoferrate [12] in the interlayer have been described. In the present paper we report on the synthesis of LDHs containing Cd^{II}, Al^{III}, and Fe^{III} in the brucite-like layers with different starting Fe/Al molar ratio and with nitrate as counteranion, following the coprecipitation method at a constant pH value of 8. Additionally, a Cd^{II},Al^{III}-LDH sample interlayered with hexacyanoferrate(III) ions was prepared by ionic exchange at pH 9. The mixed oxides obtained after calcination of Cd,Al hydrotalcites with different amounts of Fe (either in the layers or in the interlayer) have been characterized, and the effect of the initial location of iron ions on the nature and/or crystallinity of the phases formed has been also studied.

2. Experimental

2.1. Preparation of the samples

Briefly, samples containing Cd^{II}, Al^{III}, and Fe^{III} in the layers were prepared by dropwise addition of aqueous solutions in deionized water (distilled and boiled water) of the nitrates (200 mL) with different starting molar ratios ($Cd/(Al+Fe) = 2$ in all cases and $Fe/Al = 0$, 0.2, 0.7, and 1.0) into a three-neck reaction flask containing 200 mL of 1 M $NaNO_3$ aqueous solution (in deionized water) with constant stirring for 1 h; pH was kept constant at 8, using a 0.5 M NaOH aqueous solution. It was kept on stirring at room temperature for 1 h. During reaction, nitrogen was bubbled through the suspension to avoid carbonation of the samples from atmospheric CO_2. The products were submitted to hydrothermal treatment at 90 °C for 24 h, centrifuged, washed with carbonate-free water and dried at 60 °C for 24 h.

The samples were calcined at selected temperatures (see below) for 3 h in air. Samples are named as CdAlFe-N-*X*-*T*, where N stands for nitrate, *X* stands for the nominal Fe/Al molar ratio, and *T* for the calcination temperature (150, 300, 500, and 800 °C).

To prepare an additional sample containing hexacyanoferrate(III) in the interlayer, a Cd^{II},Al^{III}-nitrate hydrotalcite precursor was prepared following a method described elsewhere [6]. The solid thus obtained was filtered, washed, and suspended in decarbonated water (boiled water), and a solution (4.39 g of $K_3Fe(CN)_6$ in 100 mL of water) of hexacyanoferrate(III) was dropwise added for 1 h; pH was maintained at 9.0 to avoid precipitation of the salt. Stirring was continued at room temperature for 24 h. The precipitate was aged in the mother liquor for 24 h, filtered, washed, dried at 60 °C for 24 h, and then calcined at selected temperatures for 3 h in air. This series of samples are named as CdAl-F3-*T*, where *T* stands for the calcination temperature, in °C (same values as above for the nitrate-containing samples).

2.2. Experimental techniques

PXRD patterns were recorded in a Siemens D-5000 instrument, using Cu*K*α radiation ($\lambda = 1.5418$ Å). Diffraction lines due to the Al sample holder were recorded in some diagrams and were used as a sort of internal reference to determine more precisely the positions of the diffraction peaks. Identification of the crystalline phases has been carried out by comparison with the [14] files (5-640 for CdO, 22-1063 for $CdFe_2O_4$, and 34-71 for $CdAl_2O_4$).

Thermogravimetric (TG) and differential thermal analyses (DTA) were carried out in a Setsys Evolution 16/18 instrument from SETARAM, in flowing oxygen or N_2 (from Carburos Metálicos, Spain), at a heating rate of 5 °C min^{-1}.

The equipment used for diffuse reflectance spectroscopy was a CARY IR-UV–vis spectrophotometer. Software support for this device was the SCAN CARY v1.00 1997 from Vary Australia Pty. Ltd. Sax Software Corp.

The equipment used for magnetic susceptibility (χ) was a MS2 magnetic susceptibility system from Bartington.

Mass Spectrometry Analysis of the gases evolved during the thermal decompositions was carried out in a EM-Pfeiffer Vacuum Omnistar.

The FT-IR spectra were recorded by the KBr pellet technique in a Perkin-Elmer Spectrum One Fourier Transform instrument.

Elemental chemical analyses for Cd, Al, and Fe were carried out by atomic absorption spectrometry in an AA-3100 instrument from Perkin-Elmer.

Microstructural characterization of the materials was carried out using a JEOL JSM 6300 SEM apparatus.

3. Results and discussion

3.1. Hydrotalcite-type materials

All samples showed PXRD patterns (Fig. 1) corresponding to well-crystallized hydrotalcites with rhombohedral 3*R* symmetry [13], although for all CdAlFe-N-*X* samples very weak additional peaks corresponding to $Cd(OH)_2$ (31-228) [14] were also recorded. These peaks are also recorded in the diagram for sample CdAl-F3, together with another additional peak at $d = 3.613$ Å, assigned to $Al(OH)_3$ (37-1377) [14]. No significant change in crystallinity (as qualitatively measured from the sharpness of the peaks) is observed upon incorporation of Fe^{III} cations in the hydroxylated sheets. The first intense peak recorded close

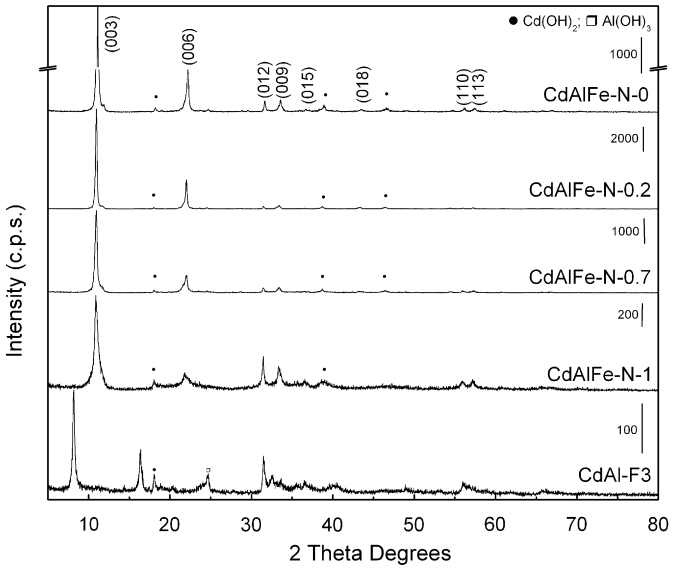

Fig. 1. PXRD diagrams of samples with nitrate in the interlayer and sample with hexacyanoferrate(III) in the interlayer.

Table 1
Lattice parameters c and a (Å) for the samples

	Sample				
	CdAlFe-N-0	CdAlFe-N-0.2	CdAlFe-N-0.7	CdAlFe-N-1	CdAl-F3
c	23.94	24.24	24.27	24.30	32.42
a	3.272	3.281	3.282	3.286	3.279

to 10° (2θ) has been ascribed to diffraction by planes (0 0 3), assuming a rhombohedral 3R symmetry [15,16]; its spacing corresponds to the height of the interlayer plus the width of a brucite-like layer. The value is in the range 7.98–8.10 Å for all samples, suggesting that the nitrate anions are located with their molecular plane parallel to the brucite-like layers [17], as for those where it is in an upwards orientation the value reported is 8.79 Å.

Crystallographic parameters a and c have been calculated by square minima fitting [18] and the values determined are included in Table 1. Parameter c corresponds to three times the spacing of the (0 0 3) peak, and increases slightly as iron is incorporated in the layers. The same trend is observed for parameter a (corresponding to the shortest metal cation–metal cation distance in the brucite-like layers). Nevertheless, the changes are rather small, and might correspond to the expansion of the structure because of the larger ionic radius of Fe^{III} than Al^{III} in octahedral coordination (0.785 and 0.675 Å, respectively) [19].

The PXRD pattern of the sample containing hexacyanoferrate(III) in the interlayer is also shown in Fig. 1, and shows the characteristics of a layered material with the hydrotalcite-like structure. Lattice parameters c and a are also included in Table 1. From the value for d(0 0 3), 10.81 Å, the thickness of the brucite-like layer (4.8 Å) [20], and the effective radius for $[Fe(CN)_6]^{3-}$ reported by Brown and Shriver [21], it can be concluded that the hexacyanoferrate unit is oriented with its C_3 axis perpendicular to the brucite-like layers, as previously reported by Kikkawa and Koizumi [22], and Braterman et al. [23] for ferrocyanide-containing Mg,Al-LDHs. The positions of the peaks are very close to those reported by other authors for Mg–Al [9,24] and Zn–Al [10] hydrotalcites intercalated with this anion. A minor contamination by $Cd(OH)_2$ and $Al(OH)_3$, as concluded from weak peaks recorded in addition to those of the layered materials, should be noticed.

Electron micrographs are shown in Fig. 2. That for sample CdAlFe-N-0 is typical of this family of layered materials, with hexagonal particles with an average particle size close to 4 μm. The particle size decreases upon incorporation of iron into the brucite-like layers, and some degree of amorphization can be also observed; the hexagonal shape of the particles is not as evident as for the iron-free samples. The electron microscopy micrograph for sample CdAl-F3 does not show flat particles, but they appear forming agglomerates.

Although sample CdAlFe-N-0 is white, the colour turns into reddish brown as the content in iron is increased, in agreement with the chromatic parameters calculated from the analysis of the diffuse reflectance spectra of the samples [25], using the MUNSELL system and shown in Table 2. For the Munsell parameters, the colour becomes red when the H-YR parameter decreases [26–28]. Sample CdAl-F3 is yellow.

Magnetic susceptibility results (χ), also included in Table 2, evidence an increase in magnetism as the amount of iron in the layers increases for the CdAlFe-N-X samples. Barrón and Torrent [29] found an increase in the magnetic susceptibility when the maghemite content in soils increases. The value measured for sample CdAlFe-N-1, with 7.27% iron (weight) can be related to that reported [30] by maghemite or magnetite, with 70% or 72% iron, respectively.

Sample CdAl-F3 is, however, diamagnetic (susceptibility $-0.005 \times 10^{-6}\,m^3\,kg^{-1}$). This result is rather surprising as configuration d^5 for Fe^{III} in the intercalated strong field anion would give rise to a system with an unpaired electron. The susceptibilities measured for the potassium salts of hexacyanoferrate(II) and hexacyanoferrate(III) are $-0.010 \times 10^{-6}\,m^3\,kg^{-1}$ and $0.080\,10^{-6}\,m^3\,kg^{-1}$, respectively (units as in Table 2).

The FT-IR spectra of the samples prepared are shown in Fig. 3; assignment of the bands is summarized in Table 3.

The samples containing nitrate in the interlayer show a very intense absorption band around 3500 cm^{-1} which is due to the stretching mode of hydroxyl groups. This band is very broad, as it involves the modes corresponding to the layer hydroxyl groups, as well as the stretching mode of interlayer water molecules. Hydrogen bonding between the water molecules and the interlayer anions also accounts for the broadening of this band. The bending mode of water

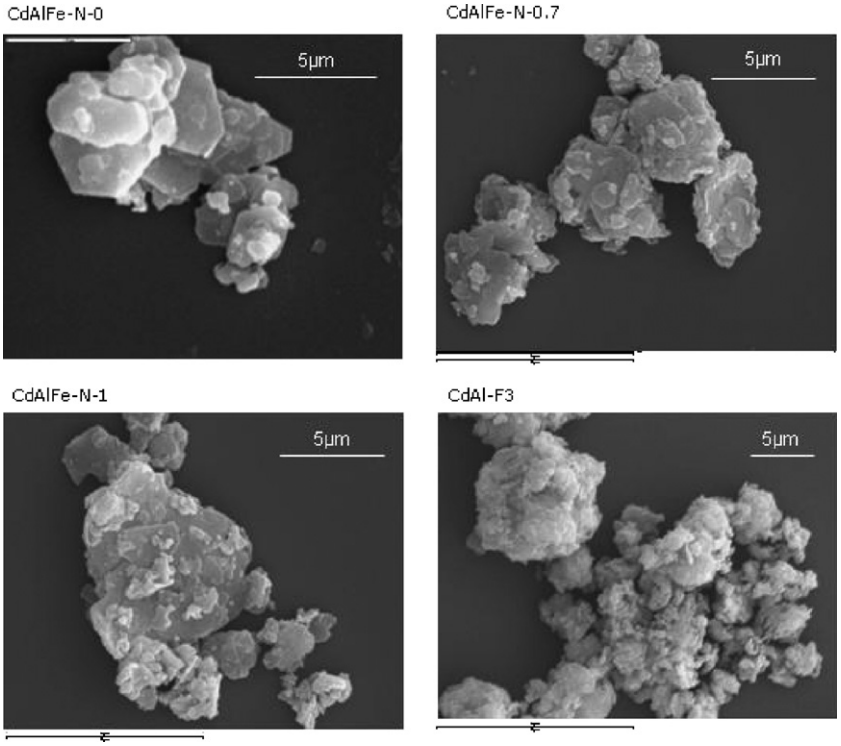

Fig. 2. SEM micrographs of samples CdAlFe-N-0, CdAlFe-N-0.7, CdAlFe-N-1, and CdAl-F3.

Table 2
Chromatic coordinates and magnetic susceptibility (χ) of the samples

Sample	χ (10^{-6} m^3 kg^{-1})	MUNSELL		
		H	*V*	*C*
CdAlFe-N-0.2	4.01	7.47YR	7.41	4.29
CdAlFe-N-0.7	15.16	5.94YR	6.35	4.97
CdAlFe-N-1	63.92	5.78YR	6.17	5.03
CdAl-F3	−0.005	1.24GY	9.05	5.40

R, red colour; Y, yellow colour; G, green colour.

gives rise to a rather weak band around 1620 cm^{-1}. The bands originated by the interlayer nitrate anions are recorded at wavenumbers somewhat lower than those corresponding to "free" nitrate anions; so the band due to mode ν_3 is recorded around 1384 cm^{-1}, while that at 827 cm^{-1} is due to mode ν_2. Mode ν_4 (680 cm^{-1} for free nitrate) is not clearly recorded, as it is overlapped by the stronger bands due to lattice vibrations. Mode ν_1 is forbidden in IR for a D_{3h} symmetry, but the IR spectrum of sample CdAlFe-N-0 shows a weak band around 1026 cm^{-1} attributed to ν_1 vibration of nitrate, together with the split ν_2 mode (826–860 cm^{-1}). The presence of a weak ν_1 band indicates a lowering of the symmetry [31], which was not indicated by Miyata [32], activating this Raman active mode. Also, a characteristic combination mode [33] $\nu_1+\nu_4$ is recorded as a weak, extremely sharp band around 1760 cm^{-1}. Finally, bands below 800 cm^{-1} are due to lattice vibrations of the brucite-like layers.

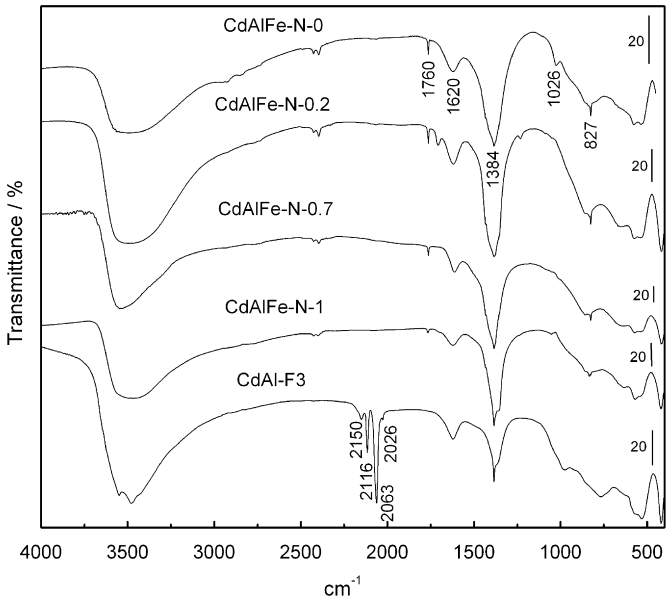

Fig. 3. FT-IR spectra of samples with nitrate or with hexacyanoferrate(III) in the interlayer.

Incorporation of hexacyanoferrate in the interlayer gives rise to four bands in the 2200–2000 cm^{-1} range, due to the stretching mode ν(CN) of the cyano ligands. However, a simple group theory analysis anticipates only a single, but triply degenerated, band for C–N stretching modes, which is recorded at 2026 and 2116 cm^{-1}, for the potassium salts of hexacyanoferrate(II) and hexacyanoferrate(III)

Table 3
Assignment of the bands recorded in the FT-IR spectra of the samples

	Sample				
	CdAlFe-N-0	CdAlFe-N-0.2	CdAlFe-N-0.7	CdAlFe-N-1	CdAl-F3
ν_{O-H}	3491	3483	3467	3467	3550, 3477
ν_{C-N}					2150, 2116, 2063, 2026
δ_{H-O-H}	1618	1619	1620	1620	1621
$\nu_3(NO_3^-)$	1384	1383	1383	1386	1384
$\nu_1(NO_3^-)$	1026	–	–	1056	
$\nu_2(NO_3^-)$	826	827	827	835	
	860	860	858	860	
$\nu_1+\nu_4$	1762	1767	1764	1768	
ν_{M-O}	578,539,426	573,539,417	575,527,419	570,534,421	570,530,419

respectively [34]. The weak band observed at 2150 cm^{-1} and the strong band [35] at 2116 cm^{-1} for the CdAl-F3 sample indicate the presence of hexacyanoferrate(III) species in the interlayer, but two additional bands around 2026 cm^{-1} (weak) and 2063 cm^{-1} (strong) indicate additional existence of hexacyanoferrate(II). This result suggests the presence of a mixture of hexacyanoferrate(III) and hexacyanoferrate(II), in the interlayer due to a reduction process from Fe(III) to Fe(II). This result is similar to that observed previously for others hydrotalcites intercalated with hexacyanoferrate(III) [9,10,34,35]. Some authors have attributed the reduction process to the pressure applied to prepare KBr discs [36] although it has been also recorded in spectra obtained using other techniques that do not require to apply pressure to prepare the samples [24]. Therefore, the mechanism of the reduction is not very clear.

Nevertheless, a small contamination by nitrate cannot be ignored, since some bands due to this anion are still recorded.

The results from elemental chemical analysis (metals) are included in Table 4. Both the raw (weight percentage) data, as well as the molar ratios, are given. Samples containing three different metal cations in the layer show a total precipitation of Al(III) and Fe(III). Nevertheless, the Cd(II)/M(III) ratio decreases when the amount of Fe(III) increases. Alternatively, this low Cd(II) content could be also seen as an excess of the trivalent cation, probably in the form of free hydroxide, but this explanation should be discarded, as no indication of crystalline by-phases is concluded from the PXRD study.

On the other hand, we expected the Cd^{II}/Al^{III} ratio in the hexacyanoferrate(III) sample being equal to 2, but the experimental value is extremely low, 1.05. The expected $Fe^{III,II}/Al^{III}$ ratio for the CdAl-F3 sample would be between 0.25 and 0.33, assuming that the only present anion in the interlayer balancing the positive charge of the layers originated by the Cd^{II}/Al^{III} substitution was hexacyanoferrate(III/II); however, the experimental value is 0.17, which seems to indicate that the layer charge is not balanced exclusively by hexacyanoferrate(III/II), in agreement with the presence of an undetermined amount of nitrate, as concluded from the FT-IR spectra.

Table 4
Elemental chemical analysis data (metals) for the samples

Sample	Cd[a]	Fe[a]	Al[a]	Cd^{2+}/M^{3+}[b,c]	Fe/Al[b]
CdAlFe-N-0	47.43	0.00	5.99	1.91	–
CdAlFe-N-0.2	49.01	2.58	5.15	1.88	0.23
CdAlFe-N-0.7	45.95	6.32	4.16	1.52	0.73
CdAlFe-N-1	38.51	7.27	3.51	1.30	1.00
CdAl-F3	40.32	3.29	9.26	1.05	0.17

[a]Weight percentage.
[b]Molar ratio.
[c]Cations in the layers.

Table 5
Formulae determined for the samples

Sample	Formula
CdAlFe-N-0	$[Cd_{0.66}Al_{0.34}(OH)_2](NO_3)_{0.34}\cdot 0.33H_2O$
CdAlFe-N-0.2	$[Cd_{0.65}Fe_{0.07}Al_{0.28}(OH)_2](NO_3)_{0.35}\cdot 0.32H_2O$
CdAlFe-N-0.7	$[Cd_{0.61}Fe_{0.16}Al_{0.23}(OH)_2](NO_3)_{0.39}\cdot 0.18H_2O$
CdAlFe-N-1	$[Cd_{0.57}Fe_{0.215}Al_{0.215}(OH)_2](NO_3)_{0.43}\cdot 0.01H_2O$
CdAl-F3	$[Cd_{0.51}Al_{0.49}(OH)_2]X^n_{0.49/n}\cdot 0.9H_2O$

$X = [Fe(CN)_6]^{3-}$, $[Fe(CN)_6]^{4-}$, and a small amount of nitrate.

The above results and the molecular water content allowed to determine the formulae included in Table 5. The sample containing hexacyanoferrate(III/II) in the interlayer has larger water content than the samples with nitrate. This fact can be attributed to the high charge of hexacyanoferrate(III/II), that entails the existence of a smaller number of anions in the interlayer, which allows to accommodate a larger amount of water molecules in the interlayer. It should be stressed that the formulae calculated are only approximate, since small amounts of $Cd(OH)_2$ in samples CdAlFe-N-X and of $Al(OH)_3$ and $Cd(OH)_2$ in sample CdAl-F3 exist and they have not been considered.

The DTA-TG diagrams of the samples with nitrate in the interlayer are very similar to each other. Diagrams for two

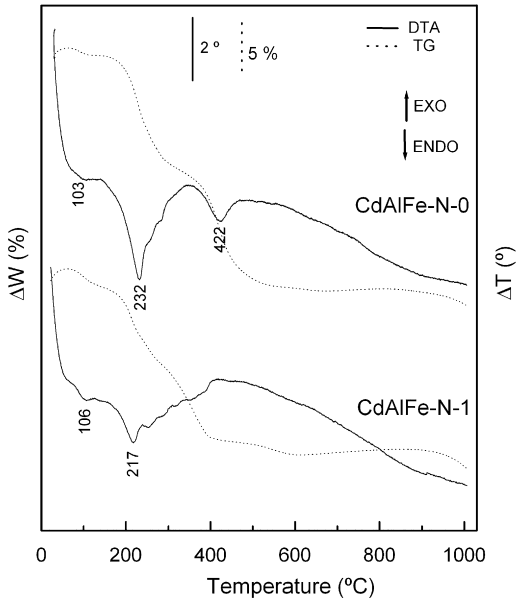

Fig. 4. TG (dotted lines) and DTA (solid lines) profiles of the samples with nitrate in the interlayer.

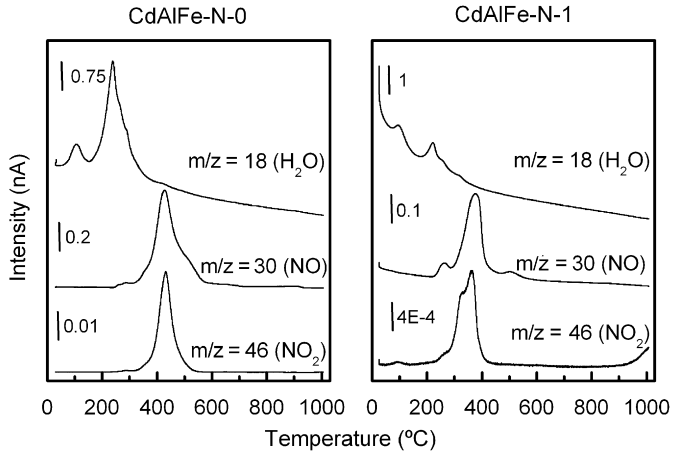

Fig. 5. Mass spectrometry diagrams of gases evolved during thermal decomposition of samples with nitrate in the interlayer.

selected samples are shown in Fig. 4. Three endothermic effects (103, 232, and 422 °C) that correspond to three mass loss are observed for sample CdAlFe-N-0. The Mass Spectrometry Analysis of the evolved gases (Fig. 5) shows that the mass loss recorded below 140 °C corresponds to removal of water, probably physisorbed on the external surface of the particles, as well as water molecules from the interlayer space. The mass loss between 140 and 320 °C corresponds to removal of water molecules formed through condensation of hydroxyl groups from the brucite-like layers giving rise to the collapse of the interlayer structure. When the Fe^{III} content in the layer of the hydrotalcite increases, the collapse of the structure takes place at a slightly lower temperature, which can be related to the larger ionic radius of Fe^{III} than Al^{III}, therefore the lower polarizing power of Fe^{III} would account for a weaker interaction with the interlayer species. The mass loss between 320 and 500 °C corresponds to removal of the interlayer nitrate ion, detected by signals at $m/z = 30$ (NO) and $m/z = 46$ (NO_2). Total mass loss (%) measured from the TG diagrams were: 24.7%, 24.8%, 22.4%, and 21.2%, for samples CdAlFe-N-0, CdAlFe-N-0.2, CdAlFe-N-0.7, and CdAlFe-N-1, respectively.

The DTA-TG diagrams recorded in air for the sample with hexacyanoferrate(III/II) in the interlayer, as well as the results from Mass Spectrometry Analysis, are shown in Fig. 6. Two endothermic effects and three exothermic effects are recorded. The two endothermic effects at ca. 155 and 258 °C are related to the loss of interlayer water and of hydroxyl groups from the layer. The three exothermic effects at ca. 330, 354, and 472 °C correspond to the pyrolysis process of hexacyanoferrate(III/II). Mass Spectrometry Analysis indicates that decomposition of interlayer hexacyanoferrate starts around 230 °C, a temperature ca. 90 °C lower than for decomposition of potassium hexacyanoferrate(III). The mass loss between 230 and 310 °C, detected by a signal at $m/z = 30$ (NO) as well as the mass loss between 310 and 500 °C, detected by signals at $m/z = 46$ (NO_2) and $m/z = 44$ (CO_2), corresponds to elimination of the interlayer hexacyanoferrate ion. Total mass loss measured in the TG diagram corresponds to 28% of the initial sample weight.

4. Calcination products

As commented above, the current interest in LDHs does not arise exclusively from their properties and chemistry, but also from the use of the products they yield upon calcination as catalysts, catalyst precursors or because of their use in devices. In order to insight in the knowledge of the crystalline phases existing in the samples after calcination, we have calcined the samples at temperatures chosen from the DTA diagrams. The samples were calcined during 3 h in air at 150, 300, 500 and 800 °C. PXRD patterns for samples with nitrate or hexacyanoferrate(III/II) in the interlayer and their calcination products at these temperatures are included in Fig. 7. The JCPDS [14] database was used to identify the crystalline phases.

At a first sight, it can be clearly seen that the behavior of the samples greatly depends on the presence of iron. On comparing the iron-free samples with those with iron in the brucite-like layers, it can be observed that the presence of this cation introduces some inestability in the layered structure, and decomposition takes place at lower temperatures. Such a change is evident even after calcination at 150 °C for sample CdAlFe-N-1, which PXRD diagram shows only very broad and weak diffraction maxima and a set of peaks in the middle of the range studied; however basal reflections are still observed in the diagrams of the other two samples when calcined at the same temperature. After calcination at 300 °C the layered structure collapses for all samples and the diffraction lines correspond to CdO

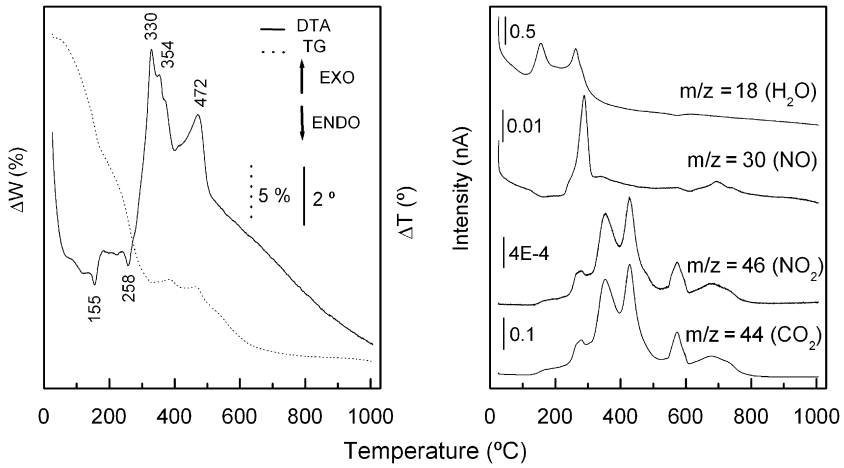

Fig. 6. TG (dotted lines) and DTA (solid lines) profiles of the samples with hexacyanoferrate(III) in the interlayer, and mass spectrometry diagrams.

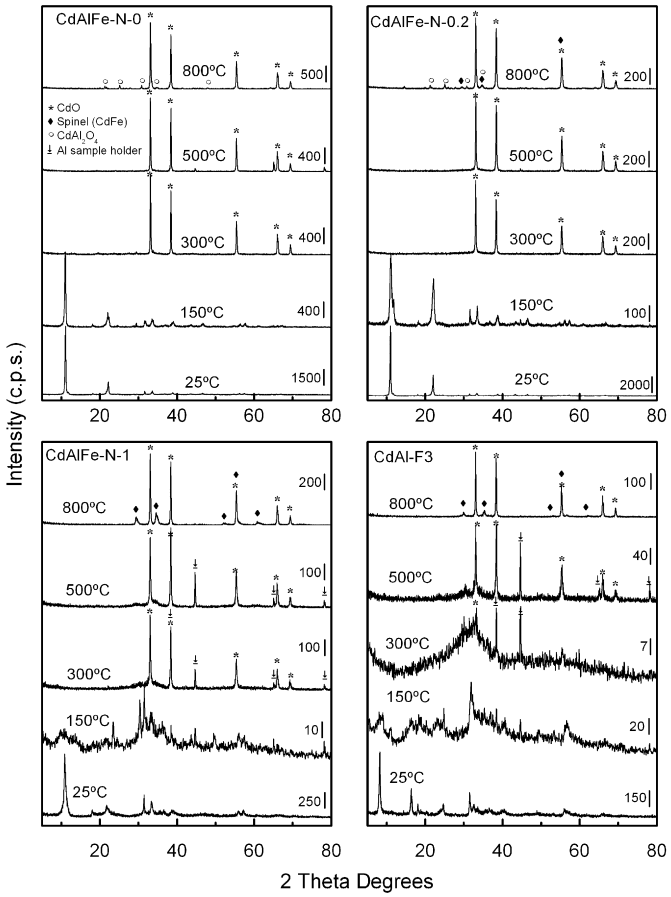

Fig. 7. PXRD diagrams of the calcined samples with nitrate or with hexacyanoferrate(III) in the interlayer at different temperatures.

(05-0640) [14] with aluminum incorporated, Cd(Al)O, with a cubic structure. This is the only crystalline phase still detected after calcining the samples at 500 °C.

Finally, the diffraction lines recorded after calcination at 800 °C correspond to Cd(Al)O and a spinel-type phase. According to the cations existing in our samples, the so-called spinel-type compound could correspond to $CdAl_2O_4$, $CdFe_2O_4$ or γ-Fe_2O_3, or to mixtures of these compounds; the presence of aluminum cannot be ruled out in these phases. As expected, due to the lack of iron, the peaks of the spinel-type material for sample CdAlFe-N-0 correspond to $CdAl_2O_4$ (34-0071) [14]. For all the other samples containing simultaneously Al and Fe a solid solution (Cd,Fe spinel) might be formed. The extreme phases will be $CdFe_2O_4$ (22-1063) [14] (Fe/Cd ratio in octahedral positions 1/1, Fe[FeCd]O_4) and γ-Fe_2O_3 (39-1346) [14] (Fe/Cd ratio in octahedral position 1.66/0, Fe[$Fe_{1.66}\square_{0.33}$]O_4). In the practise, depending on the relative amount of Cd and Fe cations in the octahedral sites, the spinel thus formed will be closer to $CdFe_2O_4$ or γ-Fe_2O_3 ($Cd_xFe_{2.66}O_4$, Fe/Cd ratio in octahedral position $1.66/x$, $0<x<0.33$). According to the PXRD patterns, two spinels coexist in calcined CdAlFe-N-0.2 and CdAlFe-N-0.7 samples, $CdAl_2O_4$ and the Cd,Fe spinel.

On the basis of these data, the process of thermal decomposition can be described in the following way:

$$\text{CdAlFe-N-0} \xrightarrow{300-500^\circ\text{C}} \text{Cd(Al)O} \xrightarrow{800^\circ\text{C}} \text{Cd(Al)O} + CdAl_2O_4$$

$$\text{CdAlFe-N-0.2/0.7} \xrightarrow{300-500^\circ\text{C}} \text{Cd(Al)O} \xrightarrow{800^\circ\text{C}} \text{Cd(Al)O} + CdAl_2O_4 + \text{spinel (Cd, Fe)}$$

$$\text{CdAlFe-N-1} \xrightarrow{300-500^\circ\text{C}} \text{Cd(Al)O} \xrightarrow{800^\circ\text{C}} \text{Cd(Al)O} + \text{spinel (Cd, Fe)}$$

On the other hand, it should be also noticed that in the diagrams for these samples the peaks corresponding to CdO appear at slightly smaller spacings than that reported in the literature, giving a value of a parameter of 4.6860 Å, lower than that expected for pure CdO ($a = 4.6953$ Å) (05-0640) [14], which might suggest the presence of aluminum cations dissolved in the CdO lattice, similarly to the data reported by Sato et al. [37], who have observed the formation of a Al–MgO solid solution during thermal

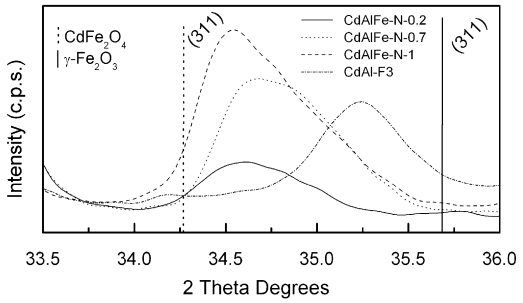

Fig. 8. PXRD diagrams of samples calcined at 800 °C. The positions of peaks due to phases $CdFe_2O_4$ (doted vertical lines) and γ-Fe_2O_3 (solid vertical lines) have been included.

decomposition of a Mg,Al-carbonate hydrotalcite at intermediate temperatures. However, both Sato et al. [37] as well as Hibino et al. [38], have shown that for their samples calcined at 800 °C the peaks are recorded in the expected positions for MgO, while in our case they are still shifted with respect to the positions expected for CdO. Finally, only one spinel-type (Cd,Fe) material is detected for sample CdAlFe-N-1.

Summarizing, incorporation of Fe^{III} in the layers gives rise to the formation of a spinel-type structure rich in this metal, as detected after calcination at 800 °C. The $CdAl_2O_4$ spinel is only observed for the samples with lower Fe^{III} content.

The PXRD diagrams recorded after thermal decomposition of the sample with hexacyanoferrate(III) are also included in Fig. 7. After calcination at 150 °C the layered structure seems to be stable, but poorly crystalline. When the calcination temperature is increased up to 300 °C the layered structure collapses and the PXRD diagram shows broad diffraction lines that indicate that the phases are poorly crystallized. Upon calcination at 500 °C more crystalline phases should be formed, and peaks corresponding to CdO are observed. The diffraction diagram of the sample calcined at 800 °C shows, together with peaks due to CdO, others corresponding to spinel (Cd,Fe). This suggests a decomposition outline similar to that shown for sample CdAlFe-N-1.

A narrow range (33.5–36.0° 2θ) diffraction diagrams for all samples, but recorded at a slower scanning rate (0.15° $2\theta\,min^{-1}$) for a more precise location of the peaks, is shown in Fig. 8. Vertical lines in this figure indicate the expected positions for the most intense diffraction peaks (3 1 1) of $CdFe_2O_4$ and γ-Fe_2O_3. The lines recorded for all CdFeAl-N-X samples are rather close to those for $CdFe_2O_4$, although slightly shifted towards lower spacing values (larger diffraction angles). In other words, these calcined solids are formed by a ($Cd_{1-x}Fe_{2+x}O_4$) spinel with more iron and less cadmium than those existing in $CdFe_2O_4$. However, the position of diffraction lines for the sample with iron in the interlayer suggests the formation of a (Cd,Fe) spinel with composition closer to γ-Fe_2O_3, but containing Cd in its structure ($Cd_xFe_{2.66}O_4$).

It should be also noticed that samples with a similar iron content, in the layer (CdFeAl-N-0.2, 2.58%) or in the interlayer (CdAl-F3, 3.29%), lead to different products when they are calcined at the same temperature: in the first case a spinel with a composition close to $CdFe_2O_4$ is formed, but in the second case the composition of the spinel is closer to γ-Fe_2O_3.

5. Conclusions

LDHs with the hydrotalcite-like structure, containing cadmium and aluminum, and with iron located in the layer (partially substituting Al cations) or in the interlayer, as a hexacyanoferrate(III) anion, have been prepared. The thermal study evidences a loss of stability and crystallinity of the layered structure as the iron content in the layer is increased. Samples with similar iron content are slightly more stable if it is located in the interlayer than in the layer. Calcination at 800 °C leads to formation of cubic CdO and spinels, formulated as $CdAl_2O_4$, $Cd_{1-x}Fe_{2+x}O_4$, and $Cd_xFe_{2.66}O_4$.

This allows that the calcination products are determined both by the iron content as well as by its location in the structure.

Acknowledgments

This work has been partially supported by MEC Projects MAT2003-06605-C02 and AGL2005-05063-CO2-02, and Junta de Andalucía through Research Group FQM-214.

References

[1] A. de Roy, C. Forano, K. Malki, J.P. Besse, in: M.L. Occelli, H.E. Robson (Eds.), Synthesis of Microporous Materials, vol. 2, Expanded Clays and other Microporous Systems, Van Nostrand Reinhold, New York, 1992, p. 108.
[2] F. Cavani, F. Triffiro, A. Vaccari, Catal. Today 11 (1991) 173.
[3] F. Triffiró, A. Vaccari, in: J.L. Atwood, D.D. MacNicol, J.E.D. Davies, F. Vögtle, J.M. Lehn, G. Alberti, T. Bein (Eds.), Comprehensive Supramolecular Chemistry, vol. 7, Pergamon Press, Oxford, 1996, p. 251.
[4] A. Vaccari, Catal. Today 41 (1998) 53.
[5] V. Rives, M.A. Ulibarri, Coord. Chem. Rev. 181 (1999) 61.
[6] D.G. Klissurski, E.L. Uzunova, Chem. Mater. 3 (1991) 1060.
[7] H. Aramendiz, G. Aguilar, P. Salas, M.A. Valenzuela. Proceedings of the 12th Iberoamerican Symposiun on Catalysis, Rio de Janeiro, Brasil, 1990.
[8] F.M. Vichi, O.L. Alves, J. Mater. Chem. 7 (1997) 1631.
[9] M.J. Holgado, V. Rives, M.S. Sanromán, P. Malet, Solid State Ionics 92 (1996) 273.
[10] I. Crespo, C. Barriga, V. Rives, M.A. Ulibarri, Solid State Ionics 101–103 (1997) 729.
[11] C. Barriga, F. Kooli, V. Rives, M.A. Ulibarri, in: M.L. Occelli, H. Kessler (Eds.), Synthesis of Porous Materials. Zeolites, Clays and Nanostructures, Marcel Dekker, New York, 1997, p. 661.
[12] I. Crespo, C. Barriga, M.A. Ulibarri, G. González-Bandera, P. Malet, V. Rives, Chem. Mater. 13 (2001) 1518.
[13] A.S. Bookin, V.A. Drits, Clays Clay Miner. 41 (1993) 551.
[14] Joint Committee on Power Diffraction Standard-International Centre for Diffraction Data, Swarthmore, PA, 1995.

[15] V.A. Drits, R.S. Bookin, in: V. Rives (Ed.), Layered Double Hydroxides: Presents and Future, Nova Science Publisers, New York, 2001, p. 39.
[16] D.M.P. Mingos, Structure and Bonding, Springer, Berlin Heidelberger, 2006.
[17] S. Miyata, Clays Clay Miner. 31 (1983) 305.
[18] J. Rodríguez-Carvajal, Program of Structure Fitting, AFFMA, 1987 version PC.
[19] J.E. Huheey, E.A. Keiter, R.L. Keiter, Inorganic Chemistry, Principles of Structure and Reactivity, fourth ed., Harper Collins College Publishers, New York, 1993.
[20] T. Kwon, G.A. Tsigdinos, T.J. Pinnavaia, J. Am. Chem. Soc. 110 (1988) 3653.
[21] D.B. Brown, D.F. Shriver, Inorg. Chem. 8 (1969) 37.
[22] S. Kikkawa, M. Koizumi, Mater. Res. Bull. 17 (1982) 191.
[23] P.S. Braterman, C. Tan, J. Zhao, Mater. Res. Bull. 29 (1994) 1217.
[24] C.B.H. Hansen, B.C. Koch, Clays Clay Miner. 42 (1994) 170.
[25] J.M. Fernández, J.A. Fernández, Color Res. Appl. 30 (2005) 448.
[26] G. Wyszecki, W.S. Stiles, Colour Science. Concepts and Methods, Quantitative Data and Formulae, Wiley, 1982.
[27] V. Barrón, J. Torrent, J. Soil Sci. 37 (1986) 449.
[28] J. Torrent, V. Barrón, in: J.M. Bigham, Ciolkosz (Eds.), Laboratory Measurement of Soil Color: Theory and Practice, Soil Science Society of America Special Publ. 31, Madison, 1993, pp. 21–33.
[29] V. Barrón, J. Torrent, Geochim. Cosmochim. Acta 66 (2002) 2801.
[30] J. Dearing, Environmental Magnetic Susceptibility, Chi Publishing, Kenilworth, England, 1999, p. 38.
[31] J.T. Kloprogge, in: J.T. Kloprogge (Ed.), The Application Of Vibrational Spectroscopy To Clay Minerals And Layered Double Hydroxides, CMS Workshop Lectures, vol. 13, The Clay Mineral Society, Aurora, CO, 2005, p. 203.
[32] S. Miyata, Clays Clay Miner. 23 (1975) 369.
[33] K. Nakamoto, Infrared and Raman Spectra of Inorganic and Coordination Compounds, Wiley, New York, 1986.
[34] S. Idemura, E. Suzuki, Y. Ono, Clays Clay Miner. 37 (1989) 553.
[35] J.T. Kloprogge, M. Weier, I. Crespo, M.A. Ulibarri, C. Barriga, V. Rives, W.N. Martens, R.L. Frost, J. Solid State Chem. 177 (2004) 1382.
[36] H.A. Larsen, H.G. Drickamer, J. Phys. Chem. 61 (1957) 1249.
[37] T. Sato, K. Kato, T. Endo, M. Shimada, React. Solids 2 (1986) 253.
[38] T. Hibino, Y. Yamashita, K. Kowge, A. Tsunashima, Clays Clay Miner. 43 (1995) 427.